COMPDYN 2023
9th ECCOMAS Thematic Conference on
Computational Methods in Structural Dynamics and Earthquake Engineering
M. Papadrakakis, M. Fragiadakis (eds.)
Athens, Greece, 12-14 June 2023

A PROCEDURE FOR THE PROBABILISTIC ASSESSMENT OF MASONRY STRUCTURES UNDER TSUNAMI

Panagiotis G. Asteris[1], Marco F. Ferrotto[2], and Liborio Cavaleri[2]

[1] School of Pedagogical and Technological Education
PC 15122 Marousi, Athens, Greece
e-mail: panagiotisasteris@gmail.com

[2] Department of Engineering, University of Palermo
Viale delle Scienze, 90128, Palermo, Italy
{liborio.cavaleri,marcofilippo.ferrotto}@unipa.it

Abstract

Assessment of Tsunami vulnerability of coastal buildings has gained high interest in the last years for the areas characterized by a high Tsunami hazard. A probabilistic representation of vulnerability is performed by fragility curves, fundamental tools to define possible strategies for risk mitigation. Different prediction approaches can be used for obtaining analytical fragility curves. In this paper, a prediction proposal to be used for masonry structures typical of the Mediterranean coasts based on simplified structural analyses and damage indexes is presented. Different damage states are considered and inundation depth is assumed as input intensity measure. The uncertainties in the demand by the definition of the probability distribution of the inundation scenarios are considered. Further, the uncertainties in the structural capacity are included. Monte Carlo simulations are performed for the scope of this work.

Keywords: Tsunami loads, vulnerability, fragility curves, tsunami fragility functions, masonry structures

1 INTRODUCTION

Tsunamis are among the most destructive events, often associated to a wide loss of human lives and wide damage to constructions, so strategies for the risk assessment need to be defined for a large scale analysis of the coastal areas [1].

In the past, earthquakes-induced tsunami events have devastated coasts causing many deaths. Among the most known there are the tsunamis of Colombian Pacific coast in 1906 and 1979, caused by earthquakes of magnitude of 8.8 and 7.6, of Japan in 1993 caused by a seismic event of magnitude of 7.7, and then the events of Indian Ocean in 2004, Samoa in 2009, Chile in 2010, Japan in 2011 caused by earthquakes of magnitude between 8 and 9.3, and of Indonesia in 2018 caused by an earthquake of magnitude 7.5. However, in some cases, tsunamis are caused by costal or underwater landslides as well (for example the Alaska tsunami in 1958).

Historically, the Mediterranean costs experienced catastrophic tsunamis: in 365 A.D. an earthquake with epicenter close to the Crete island was followed by a tsunami that caused 50.000 deaths along the costs of Egypt, Greece, Sicily and Palestine; in 1169, 20.000 deaths were counted along the costs around Catania because of a tsunami; in 1693 a tsunami caused over 60.000 deaths in Italy and Greece; in 1783 a tsunami caused about 2000 deaths in the Sicilian costs of Messina and Reggio Calabria; in the same costs in 1908 a tsunami caused waves up to 12 m height.

Different levels of vulnerability can be recognized for the different types of constructions [2] and fragility curves, very much used for seismic actions, are powerful tools to represent it by the probabilistic point of view, providing the probability of an effect (damage) due to an external action whose intensity measure (IM) is assigned. In the case of tsunami, different physical quantities are used to attribute an IM (for example the inundation depth or the momentum flux, or the Froude Number or again the flow velocity [3]), although the use of the inundation depth is more generally employed [4-7].

Different authors (e.g. [8-18]) have faced the problem of obtaining a fragility curve for different classes of constructions. However, no analytical fragility functions for masonry buildings seem that have been proposed until now. Therefore, here, a proposal for providing analytical fragility curves for masonry structures typical of Mediterranean coasts based on local analyses and local damage indexes is discussed. The proposal considers the various uncertainties in the load demand by the definition of different scenarios, and the uncertainties in the structural capacity. The fragility related to each fixed damage state is represented assuming the Tsunami inundation depth for assigning an intensity measure. Comparisons with available empirical fragility curves are presented at the end of the paper.

2 TSUNAMI HAZARD AND BULDING CHARACTERISTICS IN THE MEDITERRANEAN COSTS

Recently, the Italian National Institute of Geophysics and Volcanology (INGV Italy) carried out a tsunami hazard analysis of the Mediterranean coasts, selecting 47 points of interest and providing onshore and offshore tsunami hazard curves for an exposure time of 50 years. It was found a high variability of possible values of maximum inundation heights (MIH) depending on a probability of exceedance (PoE) in a range of 10^{-6}-10^{0}. In detail, the range of MIH covers values up to 26 meters (PoE=10^{-6}); assuming a reasonable tsunami return period of 2500 years [19], the maximum inundation heights range is between 0.6 and 6.4 m (the lowest MIH values related to the points of study in the North-West coast, the highest values related to the South-East coast).

Masonry structure buildings are widely diffused in the Mediterranean area. This is true as in the hinterland as in the coast. One of the typical costal touristic villages in the Sicilian South-Est cost is Marzamemi. The village is surrounded by the Ionian Sea (Fig. 1) and the historic center is mainly constituted by old masonry buildings. The masonry constructions considered in the present study are simple ancient constructions of one, two or at most three elevations, with wooden or reinforced concrete slabs (Fig. 2). Limestone masonry has been identified as the main construction material and the structures present poor effectiveness of the connections between the masonry walls. Several in site surveys were carried out to identify building typologies for large scale analyses.

Figure 1: Marzamemi village, Sicily

Figure 2: Typical masonry buildings in Marzamemi.

In details, three structural typologies were identified. The typology M1, consisting of ancient small single-elevation masonry buildings used as residential buildings and medium-sized buildings for commercial use, with wooden floors (flat or sloping roofs) and interstory distance of 4-6 meters. This type of buildings is used by residents or has been adapted to provide accommodation for tourists or for commercial activities.

The M2 type, consisting of small residential buildings with one elevation, more recent than the M1 type and having reinforced concrete slabs and interstory height of 3-4 meters. Finally,

the M3 type, consisting of residential masonry buildings with two or more stories and reinforced concrete slabs and interstory height of 3-4 meters. No particular differences were observed in the response of buildings with two or three floors, therefore they were grouped in a unique typology. The building typology classification is schematized in Fig. 3.
The capacity models defined for the evaluation of the structural member response under tsunami loads have been identified by the in-plane and out-of-plane behavior with respect to the shear and the flexural capacity.

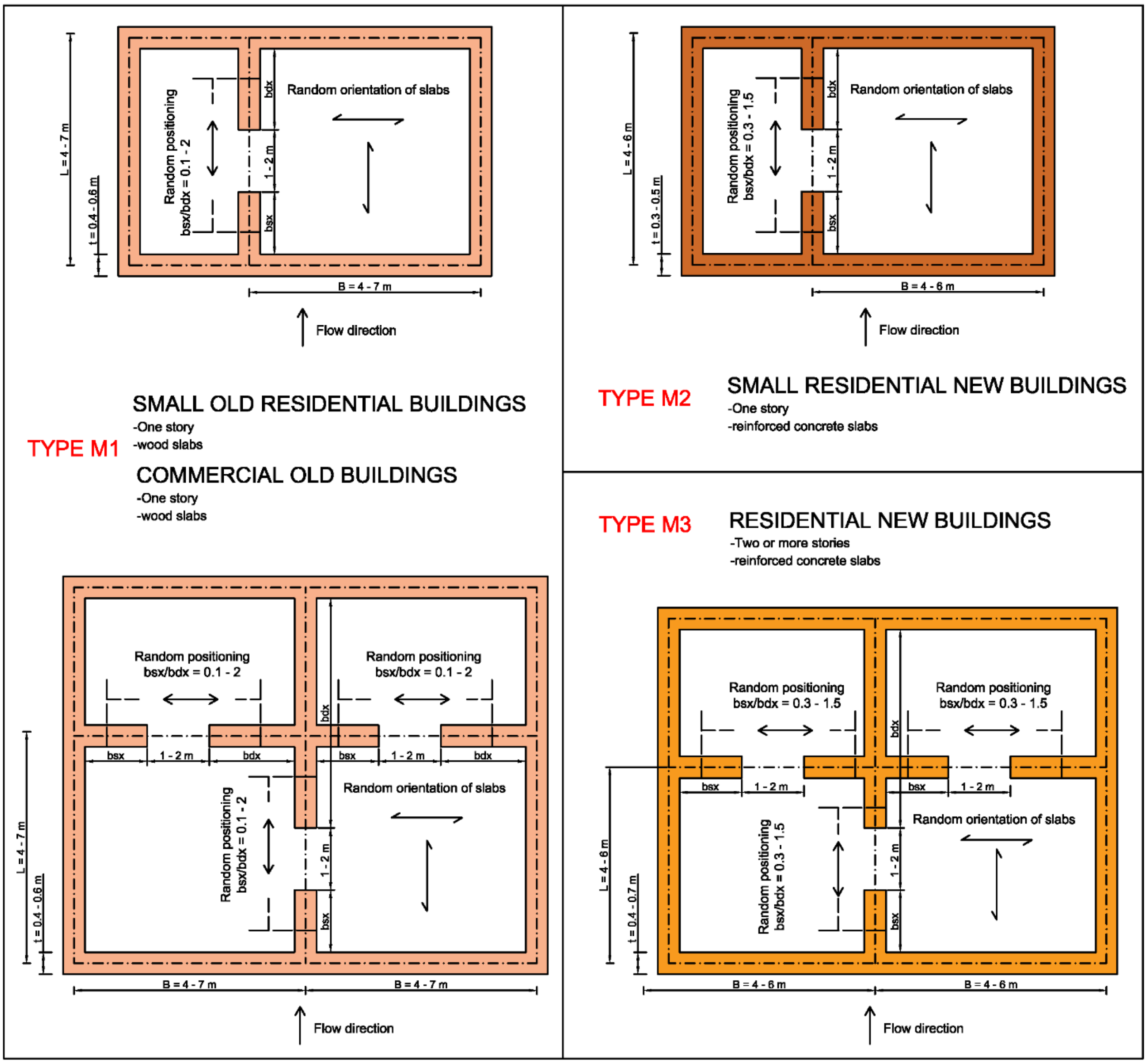

Figure 3: Masonry building typologies.

3 FRAGILITY REPRESENTATION

The term fragility in structural engineering refers to the probability of exceedance of a damage state under the expected value of an external input. Therefore, fragility functions are cumulative distribution functions that represent the probability of exceedance of a damage state, generally for a class of buildings over a range of expected intensity (the expected intensity is said Intensity Measure –IM) of an external input. It is just consolidated to express a fragility function by a cumulative probability function obtained assuming the lognormal distribution not of IM of the input but of IM of the input causing the limit state, that is

$$F(IM) = P\left[DSi \middle| IM\right] = \int_0^{IM} \frac{1}{z\beta\sqrt{2\pi}} \cdot e^{-\frac{\ln(z)-\overline{\ln(IM)}}{2\beta^2}} dz \tag{1}$$

where $F(IM)$ is the fragility function, $P\left[DSi \middle| IM\right]$ means conditional probability, that is the likelihood of occurrence of DSi based on the occurrence of IM, $\overline{\ln(IM)}$ is the average of the logarithms of the Intensity Measures of the input causing the damage DSi. Further, β includes all the uncertainties, that is the log-standard deviation of the input causing the DSi, in turn depending on the uncertainties in the capacity (β_C) and in the input itself (β_D) (Karafagka et al., 2018). The log-standard deviation of the capacity (β_C) is evaluated using the capacity of each structure analyzed considering all the uncertainties, while the log-standard deviation of the input (β_D) is evaluated from the distance between the polynomial function fitting the logarithms EDP-IM (Engineering Demand Parameters – Intensity Measure) with respect to the EDP-IM pairs obtained from a Monte Carlo simulation. Finally, β is calculated as

$$\beta = \sqrt{\beta_C^2 + \beta_D^2} \tag{2}$$

4 RANDOM VARIABLES

Several approaches for the consideration of uncertainties have been used since there is not a standard methodology available in the state of the art. For example, different approaches can be found in [5] and [6]. In the present study, geometry, material properties and input were considered random variables. At the beginning, an uniform distribution was assumed for geometry and input while a Gaussian distribution was assumed for the mechanical characteristics of the materials. The capacity is dependent by the geometry and the mechanical characteristics of the material, while the demand (EDP) is dependent by input and geometry.

Random values for the flow velocity are assumed for the evaluation of the hydrodynamic and impulsive forces that depend also on the breadth of the construction in the direction orthogonal to the flow B and the opening coefficient C_O (randomly defined) as well as the hydrostatic component.

Further involved geometrical variables are the interstory height H, the length of the walls subjected to in-plane actions L, the wall thickness t, the orientation of the structure of the slabs. Pressure distribution on the structural walls are obtained depending on the inundation depth h coupled to a random value of the velocity u. Then, in-plane and out-of-plane forces (bending moment, shear) are obtained considering hydrostatic and hydrodynamic components on one hand and impulsive component on the other hand (this two group of forces occur in two different moments of the phenomenon). The highest forces are assumed among the two cases. Capacity is obtained considering uniform randomly distributed thickness of the walls and normal distribution of the mechanical characteristics of the masonry such as the compressive and shear strengths. Subsequently, regression analysis of the demand (logarithm of inundation depth – EDP pairs) is performed for each capacity model and the median values of logarithms of the inundation depth associated to a damage state (capacity) are obtained. Then, fragility curves are obtained considering the log-standard deviation of the demand and the capacity for each damage state considered.

5 TSUNAMI INDUCED LOADS

According to standard code as ASCE/SEI 7-16 [20] and FEMA P646 [21], a Tsunami wave against an obstacle generates different forces including impact of water, hydrodynamic action, impact of debris and debris damming force. In addition, buoyancy and uplift forces should be considered as well as water retained at elevated floors.

These forces occur not at the same time, however, the above standard codes suggest how to combine them to be applied to the overall structure and to individual structural components. Other studies provided an analytical formulation for the definition of the hydrodynamic forces by equations validated by experimental testing. From the available studies, high variability in the models for the assessment of forces is observed. The problem is mainly related to the estimation of the flow velocity that causes, for a given inundation depth, a wide range of possible tsunami forces.

Here, it is proposed to evaluate the Tsunami actions according to FEMA P646, considering the total force as a sum of the hydrostatic (*Fh*) and the hydrodynamic (*Fd*) components resulting from a given inundation depth and a flow velocity as expressed in the following equations:

$$\begin{aligned} Fh &= 0.5 B\, C_O\, \rho\, g\, h^2 \\ Fd &= 0.5\, B\, \rho\, C_O\, C_D\, (h u^2) \end{aligned} \tag{3}$$

In Eq. 3, B is the breadth of the building member orthogonal to the flow, ρ is the fluid density including sediments (assumed 1100 kg/m^3), g is the gravitational acceleration, h the inundation depth, C_D is the drag coefficient, C_O the opening coefficient and (hu^2) the momentum flux. The maximum flow velocity u and the maximum momentum flux (hu^2) are estimated by the following equations for a given range of the parameter k according to [7]:

$$u_{\max} = k\sqrt{2gR\left(1-\frac{z}{R}\right)},\ k_{\max} = 0.7 \tag{4}$$

$$\left(hu^2\right)_{\max} = gR^2\left(0.125 - 0.235\frac{z}{R} + 0.11\left(\frac{z}{R}\right)^2\right) \tag{5}$$

In Eq. (5), R is the Run-up and z is the height above sea level of the construction base.

Further, FEMA P646 estimates the impulsive force Fi (due to water impact) by 1.5 times the hydrodynamic force. However, as assumed also by Medina et al. [7], this coefficient can vary between 1 and 1.5 depending on the orientation of the construction with respect to the direction of the tsunami flow. Therefore, a random multiplier of the hydrodynamic force is assumed in this study, that is:

$$Fi = \alpha\, Fd, \qquad 1 \le \alpha \le 1.5 \tag{6}$$

Finally, in this study, the flow velocity and impulsive coefficient α are assumed random independent variables like the opening coefficient Co and the breadth B of the construction member orthogonal to the Tsunami flow interested by the forces in question.
The contribution of debris impact and debris damming effects are here neglected because of the high variability in the forces due to these. Moreover, buoyancy is not considered.

6 DAMAGE STATES

Different approaches can be found in the literature that consider global and local damage indexes for reinforced concrete structures [5, 7, 22]. On the best knowledge of the authors, analytical fragility functions are not available for masonry structures.

Non-structural damage, slight damage, medium damage, extensive damage, collapse or washed away constitute a scale of damages proposed by Suppasri et al. [2, 14], for empirical fragility evaluation.

In this study, it is proposed to associate the collapse state to the reaching of the capacity of the members evaluated by local approach, while the intermediate states are empirically assumed as a percentage of the ultimate conditions. In details, non-structural damage is not considered in the present study, while slight damage (DS2), moderate damage (DS3) and extensive damage (DS4) have been defined as the 10%, 40% and the 70% of the ultimate conditions associated to the collapse (DS5).

7 INTERNAL FORCES AND CAPACITY MODELS: OUT-OF-PLANE AND IN-PLANE RESPONSE OF WALLS

The behavior of a structural type of masonry building subjected to tsunami loads has been identified through a series of geometric and structural considerations that depend on the construction techniques of the area as well as on the static scheme.

Considering a structural modeling approach based on local analysis and local damage, buildings with significantly different dimensions can have a similar response according to the static scheme. In the present work, the structural schemes have been identified according to Fig. 4 and Fig 5. Buildings with regular and non-regular plan have been assessed belonging to the same typology considering the area of influence affecting the walls in the direction of impact of the tsunami waves.

Here it is proposed a simple approach based on simplified analysis schemes for which no particular software implementation is required and the solution can be obtained by fast and simple computational methods.

7.1 Out-of-plane behavior

Regarding the out-of-plane response, the structure internal forces are evaluated by applying the loads considering the area exposed to the tsunami waves according to the scheme shown in Fig. 4. Vertical ($M_{\max} - OOP_v$) and horizontal ($M_{max} - OOP_h$) bending moments at collapse were considered. According to the current Italian Building Code 2018 [23] the following equation have been used for the vertical bending capacity

$$M_{\max} - OOP_v = \left(C_O \cdot t^2 \cdot B \cdot \frac{\sigma_0}{2} \right) \left(1 - \frac{\sigma_0}{0.85 f_m} \right) \tag{7}$$

being σ_0 the compressive stress acting on the cross-section, f_m the masonry compressive strength, t the thickness, C_O the opening coefficient and B the breadth of the masonry wall exposed to the tsunami wave.

The horizontal out-of-plane bending capacity is evaluated by considering the arch effect of the masonry walls. The mechanism is characterized by the expulsion of material from the top area of the wall and the detachment of wedge-shaped bodies accompanied by the formation of oblique and vertical plastic hinges. It is the particular case in which the activation of the kinematic mechanism is due to the crushing of the masonry at the plastic hinges, for the capacity it can be assumed

$$M_{\max} - OOP_h = f_m \cdot C_O \cdot H \cdot \frac{t}{2} \cdot f; \qquad f = \frac{t}{3} \tag{8}$$

In Eq. (8), H is the height of the masonry wall, and f defines the position of the resultant of the internal forces at the end cross-sections (Fig. 4). Note that, due to the assumption of a certain percentage of opening in the walls, to consider a reduced resisting area, the opening coefficient has been assigned in the evaluation of the capacity. Further, an opening coefficient has been adopted in the evaluation of the tsunami forces. These two coefficient may be different because one depends on the inundation depth while the other one depends on the dimensions of the wall.

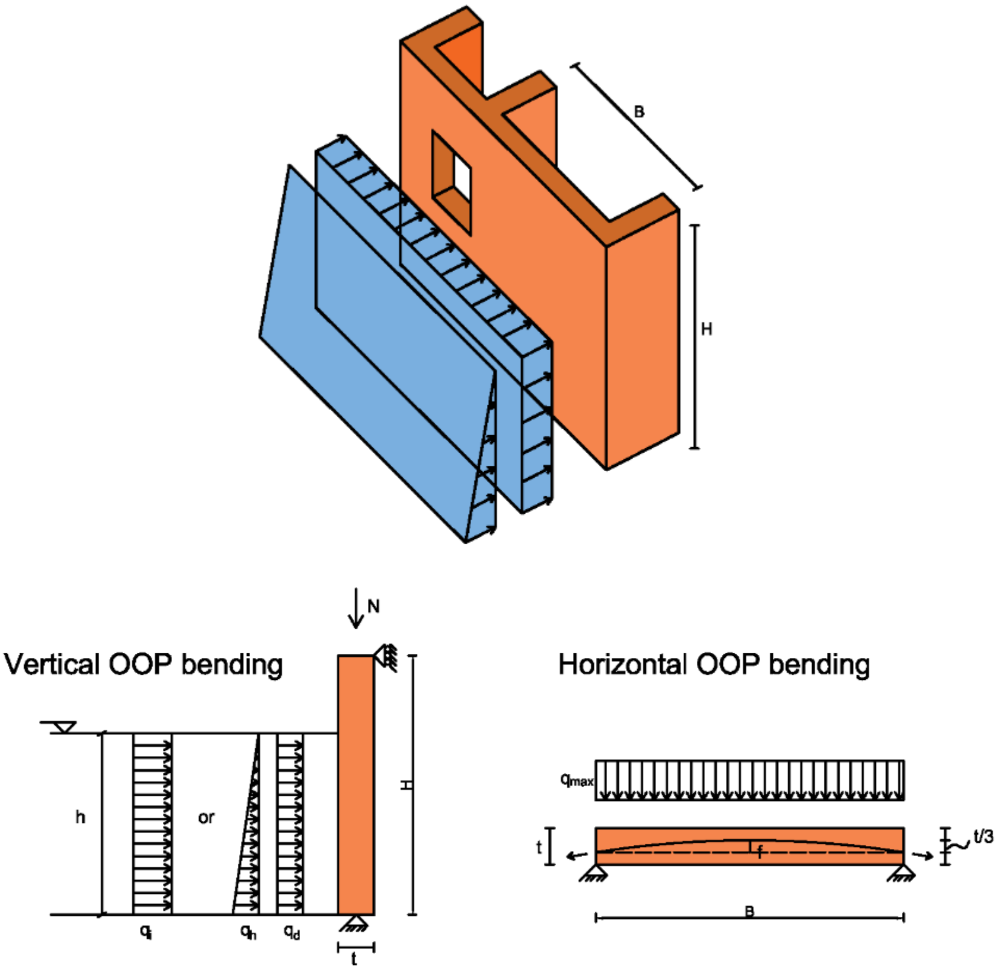

Figure 4: Analysis scheme of the evaluation of the out-of-plane response

7.2 In-plane behavior

The in-plane bending moment and shear capacities are obtained according to the scheme shown in Fig. 5. Given the pressure induced by the wave on the walls encountered out-of-plane (see again Fig. 5), it is possible to evaluate the demand in terms of in-plane shear and the in-plane bending moment in the walls not directly hit by water. Differently from the case of seismic analysis with forces applied as concentrated loads at floor level, in the case of tsunami forces, the application point of the tsunami loads depends on the inundation depth and the distribution of the forces cannot be done depending only by the stiffness of the walls. According to the scheme of Fig. 5, given two walls separated by a hole, it has been observed that the majority of shear forces are absorbed by the first wall (*bsx*) and the shear contribution in the second wall (*bdx*) are often negligible. Results of numerical parametric analyses to prove this are shown in [24].

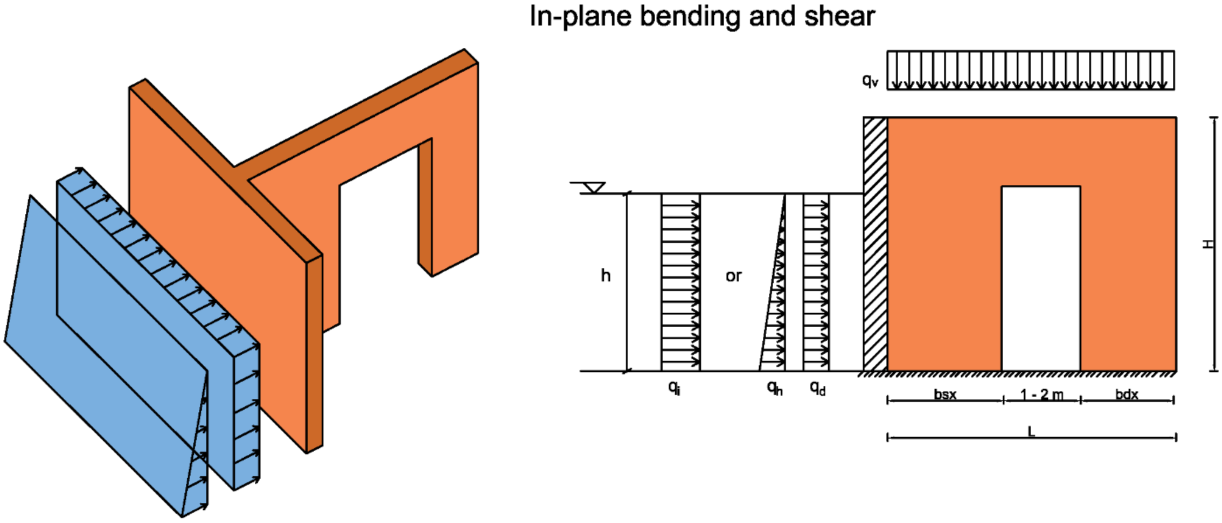

Figure 5: Analysis scheme of the evaluation of the in-plane response

The capacities in terms of bending moment and shear are derived by the equations proposed by the Italian Building Code 2018 as follows:

$$M_{\max} - IP_v = \left(C_O \cdot L^2 \cdot t \cdot \frac{\sigma_0}{2}\right)\left(1 - \frac{\sigma_0}{0.85 f_m}\right) \tag{9}$$

$$V_t = C_O \cdot L \cdot t \cdot \frac{1.5\tau_0}{b}\sqrt{1 + \frac{\sigma_0}{1.5\tau_0}} \tag{10}$$

Eq. (9) provides the bending moment capacity for a given axial load. Eq. (10) expresses the shear capacity related to the diagonal shear failure in agreement to the Turnsek-Cacovic failure criterion, τ_0 is stress corresponding to the average shear strength.

8 FRAGILITY CURVES

The aim of adopting probabilistic scenarios both for the determination of random excitations and the evaluation of the structural capacity is a common and efficient approach used by several authors [7, 25, 26].

The proposed procedure for obtaining fragility curves is based on a Monte Carlo simulation with random input, random structural geometry and random mechanical characteristics of the materials. Random variables are generated within a specific range and distribution as shown in Tab. 1.

Inundation depth range has been defined from 1 m to 4 m assuming increase intervals of 0.5 m. For each value of inundation depth h, random values of the flow velocity and the momentum flux were generated so that, for a given value of inundation depth, a number of different tsunami loads were calculated. Tsunami loads (hydrostatic, hydrodynamic and impulsive components) were also influenced by the variables B and C_O (Eq. 3). For the in-plane actions, tsunami loads were calculated depending on the area of influence and then they were applied to the walls parallel to the tsunami flow according to the scheme in Fig. 5. The presence of openings on the walls were considered assuming the values of the width: 1 m, 1.5 m or 2 m.

For each analysis case, depending on the thickness t of the walls and the compressive and shear strength of the masonry, the capacity (collapse damage state) was calculated by Eqs. 7-8 and 9-10 (some results are shown in Fig. 6 that refers to M1 type buildings).

Properties	Variables	Range/mean/standard deviation	Distribution
Geometry	B, L, t	4 m-7 m, 4 m-7 m, 0.4 m-0.6 m - (M1) 4 m -6 m, 4 m -6 m, 0.3 m-0.5 m - (M2) 4 m-6 m, 4 m-6 m, 0.4 m-0.7 m - (M3)	Uniform
	Opening coefficient C_O	0.5-1	
Materials	f_m	1.8 MPa (mean); ±0.8 MPa (standard deviation) - (M1) 2.3 MPa (mean) ± 0.9 MPa (standard deviation) - (M2-M3)	Gaussian
	τ_0	0.037 MPa (mean) ± 0.019 MPa (standard deviation) - (M1) 0.054 MPa (mean) ± 0.026 MPa (standard deviation) - (M2-M3)	
Tsunami loads	Flow velocity u	$u = 0.7\, u_{max} \div u_{max}$	Uniform
	Impact coefficient α	1 - 1.5	

Table 1: Random variable and uncertenties.

For each action, regression analysis of the logarithm of inundation depth – EDP pairs allowed the definition of polynomial fitting laws that were used for the calculation of the logarithm of the inundation depths related to the collapse damage state for a given capacity (Fig 7 refers to M2 type buildings). Each recognized logarithm of the inundation depth was assumed as median value. At this point, log-standard deviations of the demand (β_D) were evaluated calculating the dispersion of the logarithms of inundation depth - EDP simulated data with respect to the regression fit according to Karafagka et al.[5], while the log-standard deviations of the capacity (β_C) (for each capacity associated to the collapse state and therefore depending on the median values of $h_{M_{\max-OOP_v}}$, $h_{M_{\max-OOP_h}}$, $h_{M_{\max-IP}}$, h_{V_t}) were determined based on the dispersion of the results themselves (Fig. 8 refers to M1 type buildings).

For the intermediate damage states (slight, moderate, extensive) the same procedure was applied, evaluating the capacities as a percentage of that obtained at collapse.

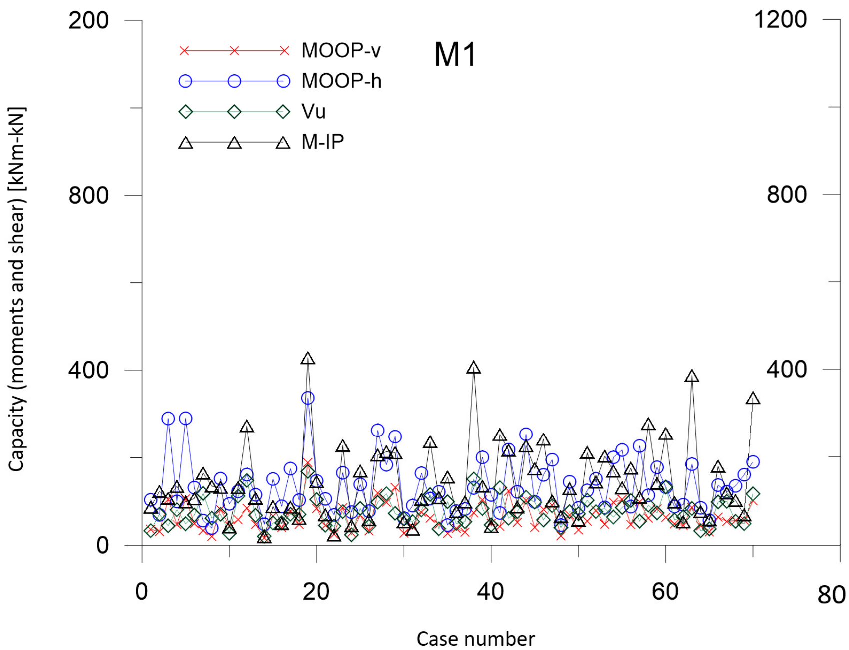

Figure 6: Capacity values obtained from different analysis cases

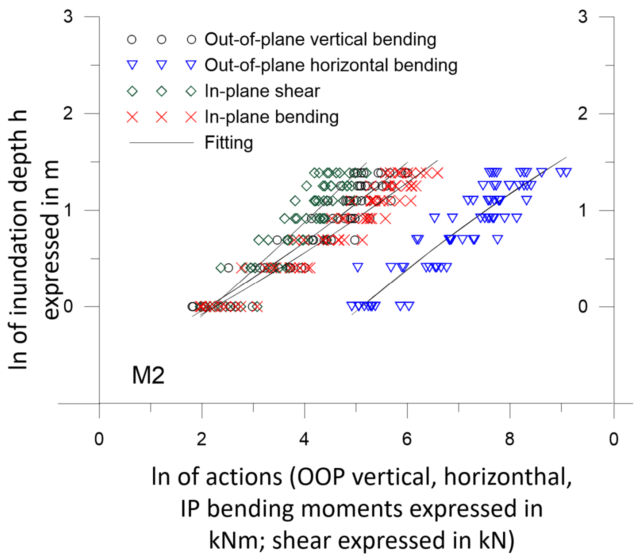

Figure 7: Logarithm of inundation depth-logarithm of internal actions pairs

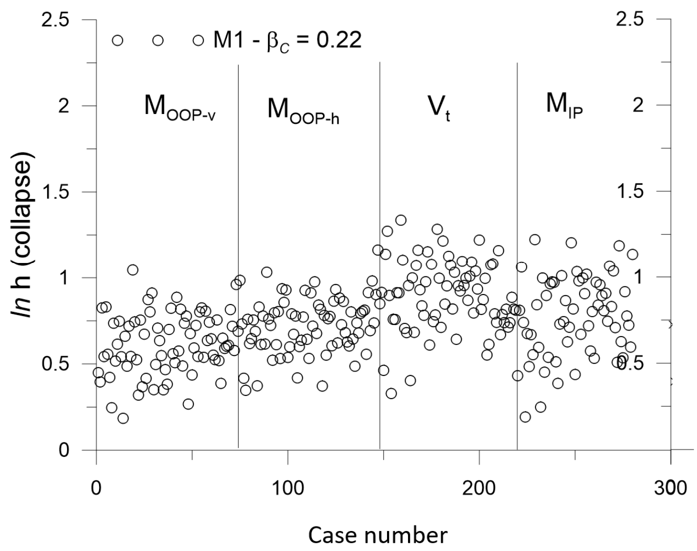

Figure 8: Logarithm of inundation depth at the collapse state.

Comparisons in terms of fragility at collapse state for the three typologies of buildings are shown in Fig. 9a.

The consistency in the results can be observed by the differences between the higher fragility expressed by the masonry type M1 with respect to the masonry type M2. Although the M1 type has walls with a thickness greater than that of the M2 type (0.4 m - 0.6 m against 0.3 m - 0.5 m), the higher mechanical characteristics of the masonry compensates for its performances. In addition, the reduced lengths of the walls exposed to the tsunami actions reduce the tsunami forces as they are related to the exposure of the building to the wave. Another substantial difference in the capacity is due to the differences in the dimensionless external axial load acting on the walls. M1 type buildings, with wooden floors, have lower dimensionless compressive stress levels compared to buildings with reinforced concrete slabs which (around 0.1 for M1 compared with around 0.2 for M2). This effect is more important in the case of buildings type M3, in which although the thicknesses is slightly higher, the normal stress level still increases (about 0.35), influencing positively their capacity. In fact, masonry buildings with two or more storey resulted much stronger (lower vulnerable) with respect to single-storey masonry at the same inundation depth. These achievements are in accordance with empirical observations available in the literature [14].

In Fig 9 b, c, d the fragility curves obtained for the four damage state considered are shown for all the masonry types.

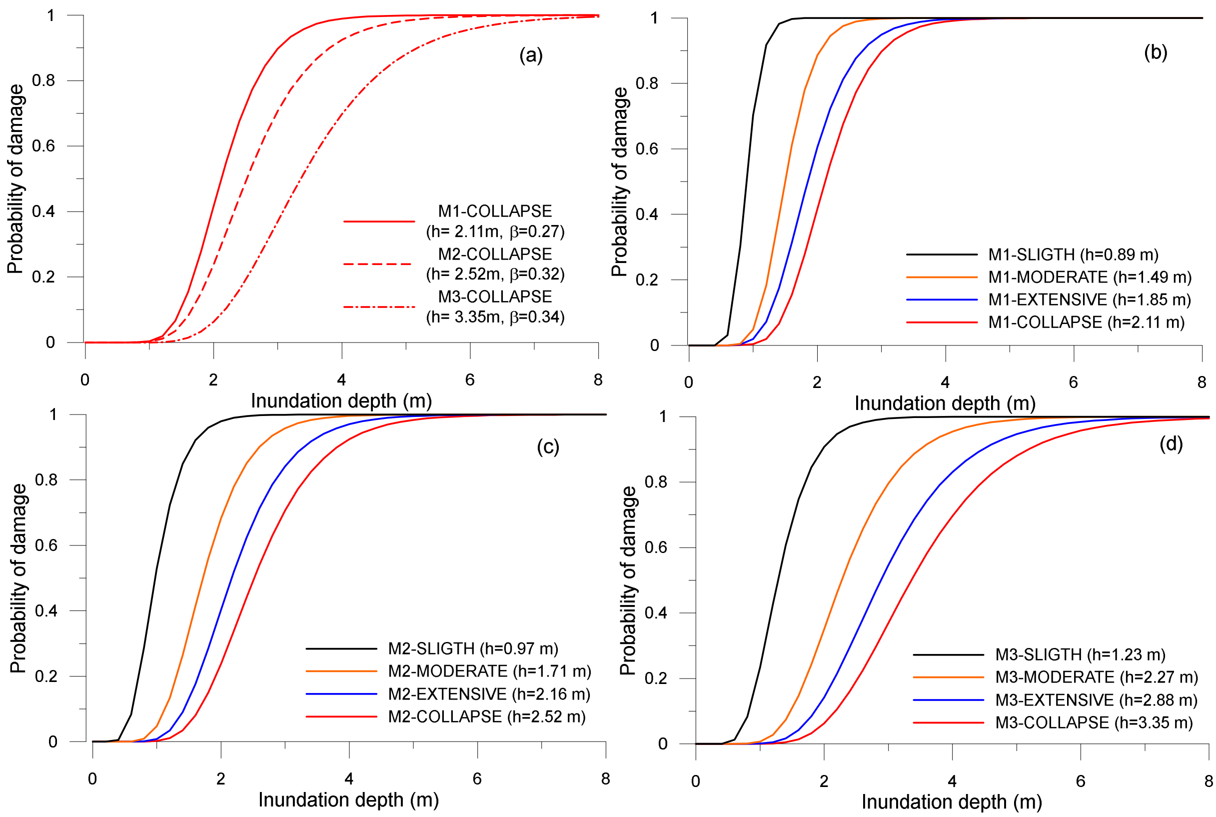

Figure 9: Fragility curves for the building typologies of Marzamemi. Comparisons at collapse state (a); Fragility at different damage state for single-storey masonry type M1 (b) and M2 (c) and multi-storey masonry type M3 (d)

9 CONCLUSIONS

In this paper, an analytical procedure for the determination of fragility curves for single-storey and multi-storey masonry buildings is presented and discussed assuming as study area a small fishing village of the Mediterranean coast, Marzamemi, Sicily. The proposed procedure is applied to a specific study area but can be generalized for other sites because the definition of tsunami forces is decoupled from specific tsunami hazard inundation scenarios. Obviously, in the case of sites different from that studied, a proper definition of the building characteristics needs. The proposed procedure allows defining the fragility curves at collapse state considering the uncertainties in the evaluation of the capacity and the demand and relates the intermediate damage state as a percentage of the capacity at collapse.

REFERENCES

[1] Unesco, *Tsunami risk assessment and mitigation for the Indian Ocean: knowing your tsunami risk and what to do about it*. IOC Manuals and Guides No. 52, Paris: UNESCO, Second edition, 2015.

[2] A. Suppasri, E. Mas, I. Charvet, R. Gunasekera, K. Imai, Y. Fukutani, Y. Abe, F. Imamura, Building damage characteristics based on surveyed data and fragility curves of the 2011 Great East Japan tsunami. *Natural Hazards*, **66**, 319–341, 2013.

[3] M.S. Alam, A.R. Barbosa, M.H. Scott, , D.T. Cox, J.W. van de Lindt, Development of Physics-Based Tsunami Fragility Functions Considering Structural Member Failures. *Journal of Structural Engineering,* **144**, 2018.

[4] C. Petrone, T. Rossetto, K. Goda, Fragility assessment of RC structure under tsunami action via nonlinear static and dynamic analysis. *Engineering Structures*, **136**, 36-53, 2017.

[5] S. Karafagka, S. Fotopoulou, K. Pitilakis, Analytical tsunami fragility curves for seaport RC buildings and steel light frame warehouses. *Soil Dynamics and Earthquake Engineering*, **112**, 118–137, 2018.

[6] K. Pitilakis, S. Argyroudis, S. Fotopoulou, S. Karafagka, K. Kakderi, J. Selva. Application of stress test concepts for port infrastructures against natural hazards. The case of Thessaloniki port in Greece. *Reliability Engineering and System Safety*, **184,** 240–257, 2019.

[7] S. Medina, J. Lizarazo-Marriaga, M. Estrada, S. Koshimura, E. Mas, B. Adriano, Tsunami analytical fragility curves for the Colombian Pacific coast: A reinforced concrete building example. *Engineering Structures*, **196**, 109309, 2019.

[8] S. Lagomarsino, S. Giovinazzi, Macroseismic and mechanical models for the vulnerability and damage assessment of current buildings. *Bulletin of Earthquake Engineering*, **4**, 415–443, 2006.

[9] V. Silva, H. Crowley, H. Varum, R. Pinho, R. Sousa, Evaluation of analytical methodologies used to derive vulnerability functions. *Earthquake Engineering and Structural Dynamics*, **43**, 181–204, 2014.

[10] I. Ioannou, J. Douglas, T. Rossetto, Assessing the impact of ground-motion variability and uncertainty on empirical fragility curves. Soil Dynamics and Earthquake Engineering, **69**, 83–92, 2015.

[11] L. Cavaleri, F. Di Trapani, M. F. Ferrotto, A new hybrid procedure for the definition of seismic vulnerability in Mediterranean cross-border urban areas. *Natural Hazards*, **86**, 517–541, 2017.

[12] P.G. Asteris, A. Moropoulou, A. D. Skentou, M. Apostolopoulou, A. Mohebkhah, L. Cavaleri, H. Rodrigues, H. Varum, Stochastic Vulnerability Assessment of Masonry Structures: *Concepts, Modeling and Restoration Aspects*. Appl. Sci., 9(2), 243, 2019.

[13] A. Suppasri, E. Mas, S. Koshimura, K. Imai, K. Harada, F. Imamura, Developing Tsunami Fragility Curves From the Surveyed Data of the 2011 Great East Japan Tsunami in Sendai and Ishinomaki Plains. *Coastal Engineering Journal*, **54**, 1–16, 2012.

[14] A. Suppasri, I. Charvet, K. Imai, F. Imamura, Fragility curves based on data from the 2011 Tohoku-Oki tsunami in Ishinomaki city, with discussion of parameters influencing building damage. *Earthquake Spectra*, **31**(2), 841–868, 2015.

[15] J. Macabuag, T. Rossetto, I. Ioannou, A. Suppasri, D. Sugawara, B. Adriano, F. Imamura, I. Eames , S. Koshimura, A proposed methodology for deriving tsunami fragility functions for buildings using optimum intensity measures. *Natural Hazards*, 84,1257, 2016.

[16] J. Macabuag, A. Raby, A. Pomonis, I. Nistor, S. Wilkinson, T. Rossetto, Tsunami design procedures for engineered buildings: a critical review. *Proceedings of the Institution of Civil Engineers – Civil Engineering* , **171**(4), 166–178, 2018.

[17] I. Charvet, J. Macabuag, T. Rossetto, Estimating Tsunami-Induced Building Damage through Fragility Functions: Critical Review and Research Needs. *Frontiers in Built Environment*, **3**, 36, 2017.

[18] P. Foytong, A. Ruangrassamee, P. Lukkunaprasit, N. Thanasisathit, Behaviours of reinforced-concrete building under tsunami loading. *The IES Journal Part A: Civil & Structural Engineering*, 2015.

[19] C. M. Rubin, B. P. Horton, K. Sieh, J. E. Pilarczyk, P. Daly, N. Ismail, A. C. Parnell, Highly variable recurrence of tsunamis in the 7,400 years before the 2004 Indian Ocean tsunami. *Nature Communications*, 8, 16019, 2017.

[20] ASCE/SEI 7-16 (American Society of Civil Engineers), *Minimum Design Loads for Buildings and Other Structures*. Reston, Virginia, 2017.

[21] FEMA. *Guidelines for the design of structures for vertical evacuation from tsunamis*. Washington, D.C.: FEMA P646, 2008.

[22] C. Petrone, T. Rossetto, K. Goda, Fragility assessment of RC structure under tsunami action via nonlinear static and dynamic analysis. *Engineering Structures*, **136**,36-53, 2017.

[23] Ministero delle Infrastrutture e dei Trasporti, *D.M. II.TT. 17.01.2018: Aggiornamento delle «Norme tecniche per le costruzioni»*, Rome, Italy, 2018 (in Italian).

[24] M. F. Ferrotto, L. Cavaleri, Masonry structures: A proposal of analytical generation of fragility functions for tsunami impact – Application to the Mediterranean coasts. *Engineering Structures*, **2421**, 112463, 2021.

[25] S. Benfratello, L. Cavaleri, M. Papia, Identification of stiffness, dissipation and input parameters of multi degree of freedom civil systems under unmeasured base excitations. *Probabilistic Engineering Mechanics*, **24**, 190-198, 2009.

[26] L. Cavaleri, M. Papia, An output-only stochastic parametric approach for the identification of linear and nonlinear structures under random base excitations: Advances and comparisons. *Probabilistic Engineering Mechanics*, **35**, 11-21, 2014.